

Mass-to-light Ratio of Ly α Emitters: Implications of Ly α Surveys at Redshifts $z = 5.7, 6.5, 7,$ and 8.8

Elizabeth R. Fernandez* and Eiichiro Komatsu

Department of Astronomy, University of Texas at Austin, 1 University Station, C1400, Austin, TX 78712

9 November 2018

ABSTRACT

Using a simple method to interpret the luminosity function of Ly α emitters, we explore properties of Ly α emitters from $5.7 \leq z \leq 8.8$ with various assumptions about metallicity and stellar mass spectra. We constrain a mass-to-“observed light” ratio, M_h/L_{band} , where M_h refers to the total mass of the host halo, and L_{band} refers to the observed luminosity of the source. For narrow-band surveys, L_{band} is simply related to the intrinsic Ly α luminosity with a survival fraction of Ly α photons, α_{esc} . The mass-to-“bolometric light”, M_h/L_{bol} , can also be deduced, once the metallicity and stellar mass spectrum are given. The inferred M_h/L_{bol} is more sensitive to metallicity than to the mass spectrum. We find the following constraints on a mass-to-light ratio of Ly α emitters from $5.7 \leq z \leq 7$: $(M_h/L_{bol})(\alpha_{esc}\epsilon^{1/\gamma})^{-1} = 21 - 38, 14 - 26,$ and $9 - 17$ for $Z = 0, 1/50,$ and $1 Z_{\odot}$, respectively, where ϵ is the “duty cycle” of Ly α emitters, and $\gamma \sim 2$ is a local slope of the cumulative luminosity function, $N(> L) \propto L^{-\gamma}$, to which the current data are sensitive. Only weak lower limits are obtained for $z = 8.8$. Therefore, Ly α emitters are consistent with either starburst galaxies ($M_h/L_{bol} \sim 0.1 - 1$) with a smaller Ly α survival fraction, $\alpha_{esc}\epsilon^{1/\gamma} \sim 0.01 - 0.05$, or normal populations ($M_h/L_{bol} \sim 10$) if a good fraction of Ly α photons survived, $\alpha_{esc}\epsilon^{1/\gamma} \sim 0.5 - 1$. We find no evidence for the end of reionization in the luminosity functions of Ly α emitters discovered in the current Ly α surveys, including recent discovery of one Ly α emitter at $z = 7$. The data are consistent with no evolution of intrinsic properties of Ly α emitters or neutral fraction in the intergalactic medium up to $z = 7$. No detection of sources at $z = 8.8$ does not yield a significant constraint yet. We also show that the lack of detection at $z = 8.8$ does not rule out the high- z galaxies being the origin of the excess near infrared background.

Key words: cosmology: early Universe, observations, theory – infrared:galaxies – galaxies:high redshift

1 INTRODUCTION

What was the universe like at high redshifts? We are currently entering a time where we can begin to observe this early time in the universe’s life by looking for galaxies at redshifts above 6.

There are several indications that stars, and hence galaxies, existed at this early time. We know that the universe was reionized early from observations such as the polarized light of the cosmic microwave background (Zaldarriaga 1997; Kaplinghat et al. 2003; Kogut et al. 2003; Page et al. 2007; Spergel et al. 2007), the Gunn-Peterson test towards quasars (e.g. Gunn & Peterson 1965; Fan et al. 2000, 2001, 2002, 2004; Becker et al. 2001; Oh & Furlanetto 2005; Goto 2006) and a gamma-ray burst

(Totani et al. 2006), and the temperature of the intergalactic medium (Hui & Haiman 2003).

In order to produce large scale reionization, an efficient and plentiful source of ultraviolet photons was needed. The first few generations of stars are very likely candidates, producing ultraviolet photons efficiently. The Ly α forest shows that the universe was polluted with metals as early as $z \sim 6$ (Songaila 2006; Pettini et al. 2003; Ryan-Weber et al. 2006; Simcoe 2006), indicating even earlier star formation and thus providing further support of early stars. In addition, a portion of the near infrared background could be the redshifted light from the first stars, and may provide information about them (Santos et al. 2002; Salvaterra & Ferrara 2003; Cooray & Yoshida 2004; Mii & Totani 2005; Madau & Silk 2005; Fernandez & Komatsu 2006; Kashlinsky et al. 2005, 2007).

It is therefore very likely that there is significant star

* beth@astro.as.utexas.edu

formation above $z > 6$. With the introduction of new, more powerful telescopes and deep field searches, an interesting question arises: do these first stars form galaxies that are bright enough to be seen today? Several deep field Ly α searches have been performed with the ISAAC on the VLT (Willis & Courbin 2005; Willis et al. 2006; Cuby et al. 2007), the Mayall Telescope at Kitt Peak (Rhoads et al. 2004), and the Subaru telescope (Taniguchi et al. 2005; Iye et al. 2006; Kashikawa et al. 2006; Shimasaku et al. 2006), probing the universe at redshifts of six and higher.

In this paper, we present a simple method to calculate the luminosity function of high- z galaxies, and compare this with the results of Ly α searches to constrain properties of Ly α emitters. In § 2, we explain our method to calculate the luminosity function of high- z galaxies with a single free parameter, a mass-to-observed light ratio, M_h/L_{band} . In § 3, we review the current generation high redshift galaxy surveys and their data. In § 4 we model stellar populations to obtain actual physical quantities about the galaxies that we observe. We compare our results to previous work in § 5 and conclude in § 6. We use the latest WMAP 3 parameters of $\Omega_b = 0.0422$, $\Omega_m = 0.241$, $\Omega_\Lambda = 0.759$, $\sigma_8 = 0.761$, $h = 0.732$, and $n_s = 0.958$ (Spergel et al. 2007).

2 A SIMPLE MODEL OF GALAXY COUNTS

2.1 Justification for a simplified approach

The simplest way to predict the cumulative luminosity function of galaxies is to count the number of haloes available in the universe above a certain mass,

$$N(> L) = V(z) \int_{M_h(L)}^{\infty} \frac{dn}{dM_h} dM_h, \quad (1)$$

where $V(z)$ is the survey volume, dn/dM_h the comoving number density of haloes per unit mass range, and M_h the total mass of a halo.

The cumulative number density of haloes, $\int_{M_h}^{\infty} dM_h dn/dM_h$, is shown in the bottom panel of Figure 1. In order to calculate the cumulative luminosity function, one may simply “stretch” the horizontal axis of this figure by dividing M_h by a suitable factor that converts the mass to luminosity: a mass-to-light ratio, M_h/L .

This model is admittedly oversimplified, and is indeed simpler than what is already available in the literature. For example, one can stretch not only the horizontal axis (i.e., mass), but also the vertical axis of the cumulative mass function as $\int dM_h dn/dM_h \rightarrow \epsilon \int dM_h dn/dM_h$, where ϵ is often called a “duty cycle” (e.g., Haiman et al. 2000).

The vertical stretch would be required when the average lifetime of Ly α emitting galaxies, τ_g , is shorter than the age of the universe, in which case the number count should be given by the time derivative of the mass function, $\int dM_h dn/dM_h \rightarrow \int dM_h \tau_g(M_h) d^2n/(dM_h dt)$. The vertical stretch parameter is thus given approximately by $\epsilon \approx \tau_g/t_{\text{univ}}$.

Since the statistical power of the current data is not yet strong enough to constrain both the horizontal and vertical stretch parameters simultaneously, these parameters are strongly degenerate (Dijkstra et al. 2006; Stark et al. 2007). They are completely degenerate when $N(> L)$ follows a sin-

gle power law, $N(> L) \propto L^{-\gamma}$. The degeneracy line is given by $(M_h/L)\epsilon^{-1/\gamma} = \text{constant}$; thus, the inferred M_h/L and ϵ are positively correlated: the smaller the ϵ is, the smaller the inferred M_h/L becomes.

In order to lift this degeneracy, therefore, it is essential to detect the deviation of $N(> L)$ from a power law. Since the cumulative mass function in $5.7 \leq z \leq 8.8$ begins to decline exponentially with mass at a few times $10^{11} M_\odot$ at $z \sim 6$ to $10^{10} M_\odot$ at $z \sim 9$ (see Fig. 1), an accurate determination of the bright end of the luminosity function at $L_{Ly\alpha} \gtrsim 10^{42} \text{ erg s}^{-1} \times (100 L_{Ly\alpha}/M_h)$ at $z \sim 9$ to $10^{43} \text{ erg s}^{-1} \times (100 L_{Ly\alpha}/M_h)$ at $z \sim 6$ would be required to lift the degeneracy. (Note that M_h/L is always quoted in units of $M_\odot L_\odot^{-1}$, where $L_\odot = 3.8 \times 10^{33} \text{ erg s}^{-1}$.) The bright end of the luminosity function is not constrained very well by the existing surveys (see Fig. 2). One would need a larger survey area for a better determination of the bright end of the luminosity function. (See section 4.1 for further discussion on constraining the bright end of the luminosity function.)

We have chosen to work with $\epsilon = 1$, which is allowed by the existing data (Dijkstra et al. 2006; Stark et al. 2007). As we show in this paper, this assumption does provide reasonable and useful results. We then use the degeneracy line, $(M_h/L)\epsilon^{-1/\gamma} = \text{constant}$, to incorporate the effect of ϵ into the inferred constraints on properties of Ly α emitters.

A further improvement to the model can be made by taking into account the fact that a relation between the luminosity and halo mass is not unique, but has some dispersion. One may include this by using a conditional probability of luminosity given the halo mass, $P(L|M_h)$, as $N(> L) = V(z) \int dM_h P(L|M_h) dn/dM_h$ with $P(L|M_h)$ given by, e.g., a log-normal distribution (Cooray & Milosavljevic 2005). Once again, the current data cannot constrain the extra parameters characterizing $P(L|M_h)$, except for its first-order moment, a mass-to-luminosity ratio. In our simplified approach we take it to be a delta function, $P(L|M_h) = \delta^D[M_h - (M_h/L)L]$, which gives equation (1).

In this paper we shall use the Sheth-Tormen formula for dn/dM_h (Sheth et al. 2001; Sheth & Tormen 2002). Since the Press-Schechter mass function (Press & Schechter 1974) tends to underestimate the number of haloes in the high mass range, the mass-to-light ratio inferred from the Press-Schechter mass function would be smaller than that from the Sheth-Tormen formula. We have found that the mass-to-light inferred from the Press-Schechter mass function is smaller by a factor of two.

The volume, $V(z)$, is found by multiplying the comoving volume element, $d^2V/dzd\Omega$, by the depth of the survey (found by integrating over redshift) and the survey area on the sky. For narrow-band surveys, the redshift integral can be approximated as Δz . The comoving volume element is given by

$$\frac{d^2V}{dzd\Omega} = \frac{cd_L^2(z)}{1+z} \left(-\frac{1}{H(z)(1+z)} \right), \quad (2)$$

where d_L is the proper luminosity distance.

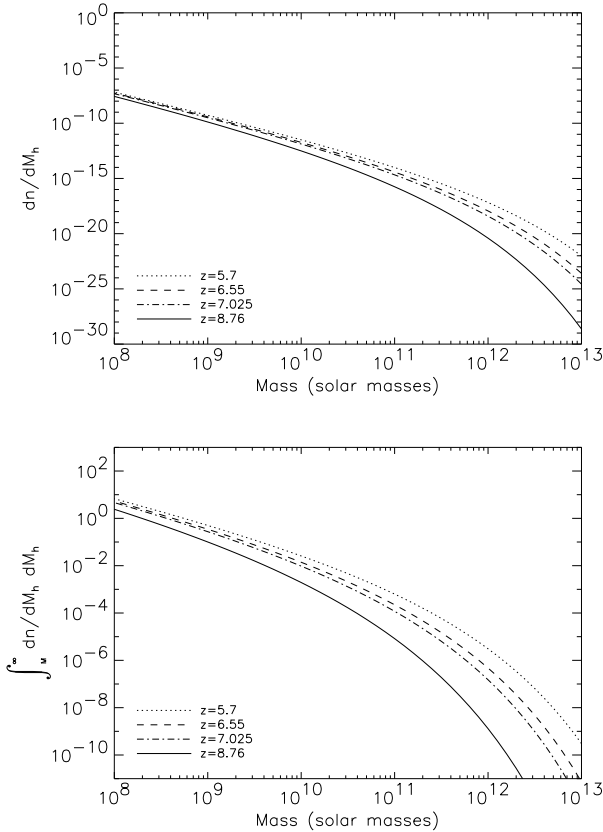


Figure 1. Mass function. The dotted, dashed, dot-dashed and solid lines show $z = 5.7, 6.55, 7.025,$ and $8.76,$ respectively. These are the redshifts of narrow-band surveys that we consider in this paper (see Table 1). (*Upper Panel*) The Sheth-Tormen mass function as a function of halo mass, $dn/dM_h,$ in units of comoving $\text{Mpc}^{-3} M_{\odot}^{-1}$ (*Lower Panel*) The cumulative mass function, $\int_{M_h}^{\infty} dM_h dn/dM_h,$ in units of comoving Mpc^{-3} . The cumulative luminosity function can be calculated by stretching the horizontal axis of this figure by dividing M_h by a suitable factor that converts the mass to luminosity: a mass-to-light ratio, M_h/L .

2.2 Basic formalism

From equation (1) we can derive the number of galaxies observed above a certain flux density as:

$$\begin{aligned} & \int_{F_{limit}}^{\infty} \frac{d^2 N}{dF d\Omega} dF \\ &= \int dz \frac{d^2 V}{dz d\Omega} \int_{F_{limit}}^{\infty} \frac{dn}{dM_h} \frac{dM_h}{dF} \vartheta(M_h - M_{min}(z)) dF \\ &\approx \Delta z \frac{d^2 V}{dz d\Omega} \int_{F_{limit}}^{\infty} \frac{dn}{dM_h} \frac{dM_h}{dF} \vartheta(M_h - M_{min}(z)) dF. \end{aligned} \quad (3)$$

where M_h is the halo mass.

Not all dark matter haloes will be forming stars - only haloes with a mass above some critical minimum mass (M_{min}). This is represented by the function $\vartheta(M_h - M_{min}(z))$, which is zero if the halo mass is smaller than M_{min} and unity if it is larger than or equal to M_{min} . The minimum mass is only theoretically known, and we use the virial mass of a 10,000 K halo, $M_{min} = 0.94 \times 10^8 M_{\odot} [(1 +$

$z)/10]^{-3/2}$. However, given the current sensitivity of telescopes, it is unlikely that a halo of mass M_{min} will be bright enough to be seen, unless the mass to light ratio of galaxies is unusually small. Therefore, M_{min} is irrelevant to our analysis presented in this paper and our conclusion is independent of the actual value of M_{min} .

In deriving equation (3), we have made an assumption that each dark matter halo above M_{min} hosts one galaxy. This is a valid assumption at high redshifts, as massive haloes such as groups ($M \gtrsim 10^{13} M_{\odot}$) and clusters ($M \gtrsim 10^{14} M_{\odot}$) of galaxies hosting multiple galaxies are extremely rare (see Fig. 1). If we were to assume a field size equal to the largest survey area discussed in this paper (that of the LALA survey, 1296 arcmin²), and the widest redshift range (that of the Subaru survey at $z \sim 7$), the number of haloes above a mass of $10^{13} M_{\odot}$ can be found by using equation 1. At a redshift of 1, there would be 32 haloes larger than this mass in the field. At higher redshifts ($z = 3, 5,$ and 7), there would be less than one such massive halo in the field ($0.98, 1 \times 10^{-3},$ and 7.7×10^{-8} , respectively.) Thus at high redshifts, it is safe to assume that there are no groups or clusters observed. (Larger surveys (Ouchi et al. 2005) have observed protoclusters). This property makes it possible to model the luminosity function of high- z galaxies without complications arising from galaxy formation processes. Some observations (i.e. Ouchi et al. (2004)) show that some dark matter haloes host more than one Ly α emitter. However, since galaxy occupation number at high redshifts is not well known, we will just assume one galaxy per halo.

The most important uncertainty in our model is that not all galaxies are seen as Ly α emitters. Some galaxies do not produce as many Ly α photons as the others do because of dust extinction in galaxies themselves and scattering in the IGM. Therefore we could have assumed that there is less than one Ly α emitter per halo; however, this effect can be modeled effectively by introducing a Ly α survival fraction, α_{esc} . This parameter quantifies the fraction of Ly α photons that escaped from a halo *and* the IGM. Therefore, as α_{esc} increases, a galaxy is seen as more luminous intrinsically.

In summary, we model the galaxy number counts by placing one galaxy per halo with only a fraction of photons escaping from galaxies and the IGM.

2.3 Mass-to-“observed light” ratio

Our formulation is now reliant on how we relate the flux density of a galaxy to its mass.

The flux density of galaxies depends on two things: the luminosity distance to galaxies, and a mass-to-“observed light” ratio, which will relate the total mass of the halo (including dark matter) to the luminosity that is actually observed. The flux density of a galaxy observed by a certain instrument is found by:

$$F = \frac{L_{band}/M_h}{4\pi d_L^2(z)\Delta\nu_{obs}} M_h, \quad (4)$$

where $\Delta\nu_{obs}$ is the bandwidth of the instrument (which we have assumed to have an ideal rectangular bandpass) and

$$L_{band} = \int_{\nu_{1,obs}(1+z)}^{\nu_{2,obs}(1+z)} d\nu L_{\nu}, \quad (5)$$

is the observed luminosity within a certain bandwidth of the instrument, L_ν the rest-frame luminosity per unit rest-frame frequency, and ν_2 and ν_1 the frequency limits of the survey.

We assume that the mass to light ratio is independent of mass, $dM_h/dF = M_h/F$. This approximation is well justified, as the current surveys are probing a limited mass range. Total and stellar masses are still unknown for Ly α emitters. Studies of the stellar masses using SED fitting have just begun (Mobasher et al. 2005; Nilsson et al. 2007). In the future when the observations of Ly α emitters can cover a wide mass range, one may use a parametrized model, e.g., $L \propto M^\beta$, to improve fits. For the present purpose additional parameters are unnecessary.

Using equation (4), equation (3) can be rewritten with respect to M_h/L_{band} :

$$\begin{aligned} & \int_{F_{limit}}^{\infty} \frac{d^2 N}{dF d\Omega} dF \\ &= 4\pi d_L^2(z) \frac{dV}{dz d\Omega} \Delta z \Delta \nu_{obs} \frac{M_h}{L_{band}} \int_{F_{limit}}^{\infty} \frac{dn(M_h(F))}{dM_h} dF \\ & \quad \times \vartheta(M_h - M_{min}(z)). \end{aligned} \quad (6)$$

To evaluate dn/dM for a given F , we use equation (4) to convert F to M_h . Once again, M_h/L_{band} is independent of M_h , and M_h is almost always greater than M_{min} , and thus almost always $\vartheta(M_h - M_{min}(z)) = 1$. The only unknown quantity in this equation is M_h/L_{band} , while $\Delta \nu_{obs}$, F_{limit} , and Δz are given by the survey properties. In other words, M_h/L_{band} is the parameter that should be measured from the observational data directly.

3 NARROW-BAND LY α SURVEYS: OBSERVATIONS

Several telescopes are now powerful enough to attempt to locate galaxies at $z \gtrsim 6$. One effective method of locating high redshift galaxies is to use narrow-band filters to detect Ly α emission from a small range of redshifts. Ly α emitters tend to have large equivalent widths, with their line intensities significantly higher than the continuum emission. In order to test that the galaxy is indeed a high redshift galaxy, it must be undetected at optical wavelengths, and follow-up spectroscopy may be employed if possible. At times, when no continuum is visible, the asymmetric profile of the Ly α line can be used to identify a Ly α emitter.

A large number of such narrow-band Ly α searches have been carried out on blank fields at $z = 5.7$ (Rhoads & Malhotra 2001; Rhoads et al. 2003; Maier et al. 2003; Hu et al. 2004; Ouchi et al. 2005; Ajiki et al. 2003, 2004, 2006; Shimasaku et al. 2006; Murayama et al. 2007), $z = 6.5$ (Kodaira et al. 2003; Taniguchi et al. 2005; Kashikawa et al. 2006), $z = 7$ (Iye et al. 2006), and $z = 8.8$ (Willis & Courbin 2005; Willis et al. 2006; Cuby et al. 2007). Kurk et al. (2004) used an alternative technique, a slitless-grism spectroscopy survey, which has also yielded a successful detection of a Ly α emitter at $z = 6.5$. Martin & Sawicki (2004) performed a multi-slit windows search at $z = 5.7$.

In this paper we use the observational data from six narrow band Ly α searches: two from the Infrared Spectrometer and Array Camera (ISAAC) on the Very Large Telescope

(VLT), three from Subaru, and one from the Mayall Telescope at Kitt Peak. The basic parameters of these surveys are summarized in Table 1.

Two surveys at $z = 5.7$ and $z = 6.56$ were taken at the Subaru telescope using the Suprime-Cam. The surveys covered 725 and 875 arcmin², respectively. These surveys had a limiting flux density of 145 nJ. Candidates were found down to a limiting magnitude of 26.0 (at a detection limit of 3σ for $z=5.7$ and 5σ for $z=6.56$) using a $2''$ aperture. At $z = 5.7$, there were 89 Ly α emitter candidates, 63 were followed up by spectroscopy, and 34 Ly α emitters have been confirmed (Shimasaku et al. 2006). At $z = 6.56$, there were 58 Ly α emitter candidates, 53 were followed up by spectroscopy, and 17 Ly α emitters have been confirmed (Taniguchi et al. 2005; Kashikawa et al. 2006). From these detections, they were able to fit a Schechter function, $\phi(L)dL = \phi^*(L/L^*)^\alpha \exp(-L/L^*)dL/L^*$, with parameters given in Table 2.

The Large Area Lyman Alpha (LALA) survey searched for galaxies at a redshift of around 6.55 (Rhoads et al. 2004). This survey was conducted on the 4-m Mayall Telescope at Kitt Peak. A narrow-band 1296 arcmin² image was taken of the Boötes field. The limiting flux density was 700 nJ. Three candidates were located down to a limiting magnitude of 24.3 (5σ) with a $1''.02$ aperture – one of which was confirmed spectroscopically as a Ly α emitter.

Another survey using the Subaru telescope covered an area of 876 arcmin² at $z = 7.025$. They used the narrow band filter NB973 on the Subaru Suprime-Cam and had a limiting flux density of 398 nJ. There were 2 Ly α emitter candidates down to a limiting magnitude of 24.9 (5σ) with a $2''$ aperture – one of which was confirmed spectroscopically as a Ly α emitter at $z = 6.96$ (Iye et al. 2006).

ZEN, which stands for z equals nine, is a narrow J-band mission using the ISAAC on the VLT. Its central redshift is 8.76 and it covers a field size of 4 arcmin² down to a limiting flux density of 302 nJ. They searched for galaxies in the Hubble Deep Field South that displayed an excess in the narrow band in comparison to the J-band ($J_s - NB \geq 0.3$) and that were undetected in the optical. No galaxies were found down to a limiting magnitude of 25.2 (5σ) with a $0''.7$ aperture (Willis & Courbin 2005; Willis et al. 2006).

Cuby et al. (2007) did a followup narrow-band search, using the ISAAC at the VLT, with a larger field of view (hereafter referred to as the ISAAC ext). They imaged seven fields in the Chandra Deep Field South that totaled 31 arcmin² down to a flux density of 1740 nJ. They also detected no galaxies within the fields down to a limiting magnitude of 23.3 (5σ) with a $1''$ aperture.

4 PROPERTIES OF LY α EMITTERS

4.1 Extracting a mass-to-“observed light” ratio

Can we infer anything about properties of the Ly α emitters discovered in these narrow-band surveys? Is the lack of detections in the fields above $z > 7$ expected, or should we expect many more galaxies?

In equation (6), the only free parameter was the mass-to-“observed light” ratio, M_h/L_{band} . Therefore, we vary M_h/L_{band} to give a model that is consistent with observations. The number of galaxies drops as M_h/L_{band} increases.

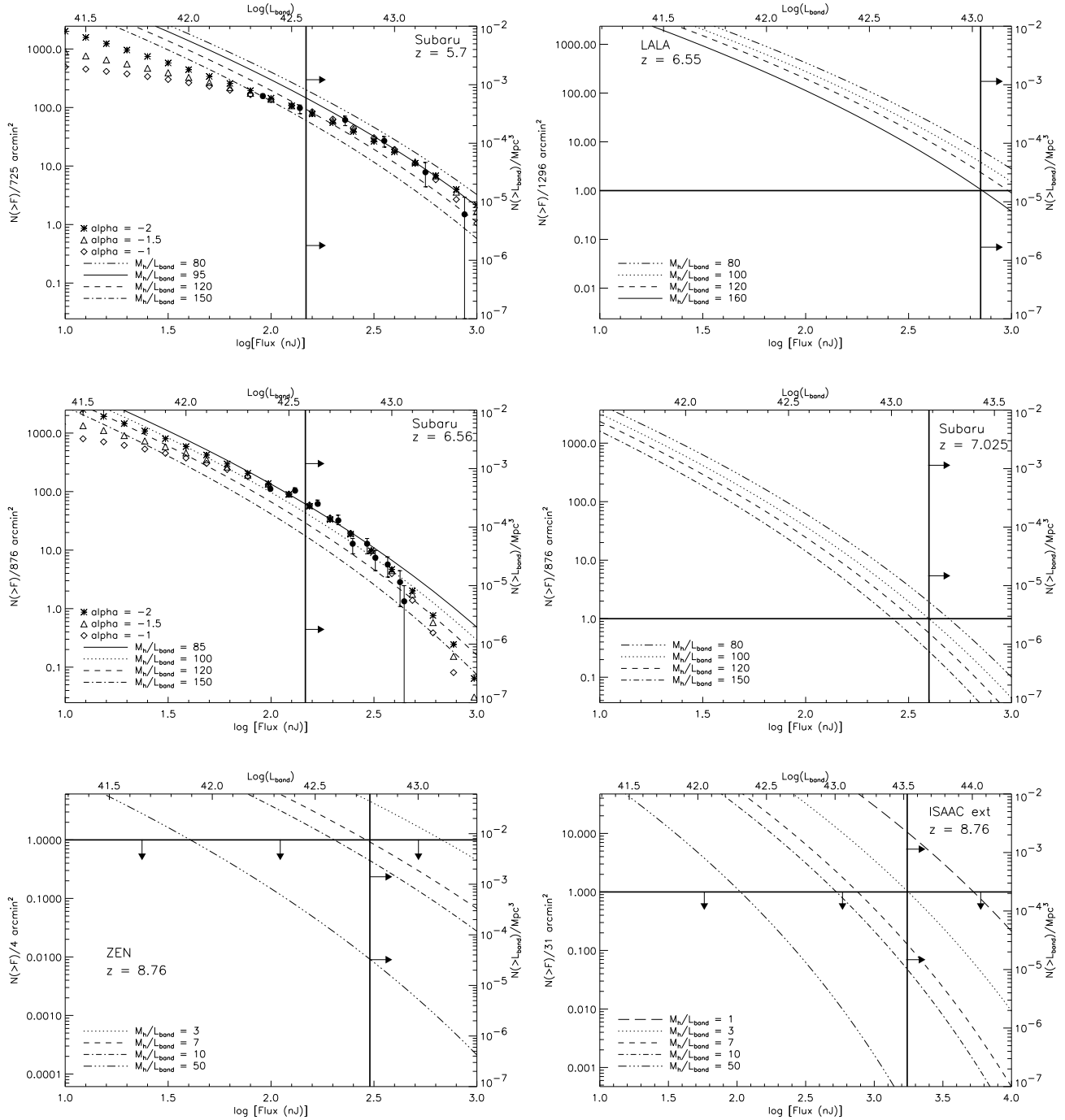


Figure 2. The observed luminosity function of Ly α emitters constrains their mass-to-“observed light” ratio. Each panel shows the cumulative number of sources detected in each field above a certain flux density, $N(> F)$. (The flux density limits of each survey are indicated by the vertical lines with right arrows.) The bottom and top axis show the measured flux density and luminosity (in erg s^{-1}), respectively, while the left and right show the number of sources per field and per comoving Mpc^3 , respectively. The mass-to-“observed light” ratio, M_h/L_{band} , is fit to each of the luminosity functions derived from various narrow-band surveys. Here, L_{band} refers to the light that falls within the band of instruments, which is mostly the Ly α line. Curves in each panel show predictions with various M_h/L_{band} . (*Upper Left*) The Subaru field at $z = 5.7$ (Shimasaku et al. 2006). The stars, triangles and diamonds show their Schechter-fit to the luminosity function with $\alpha = -2$, -1.5 and -1 , respectively. The scatter between symbols shows uncertainty, and they diverge mostly below the flux density limit, as expected. The solid circles are the data, with the error bars showing Poisson error. (*Upper Right*) The LALA field at $z = 6.55$ (Rhoads et al. 2004). One Ly α emitter was found, and the horizontal line shows $N(> F) = 1$ per field. (*Middle Left*) The Subaru field at $z = 6.56$ (Taniguchi et al. 2005; Kashikawa et al. 2006). The meaning of symbols is the same as in the upper left panel. Data is from both the photometric and spectroscopic samples. The circles show data corrected for detection completeness. (*Middle Right*) The Subaru field at $z = 7.025$ (Iye et al. 2006). One Ly α emitter was found. (*Bottom Left*) The ZEN field at $z = 8.76$ (Willis & Courbin 2005; Willis et al. 2006). No sources were found, and the horizontal line with lower arrows shows $N(> F) < 1$ per field. (*Bottom Right*) The ISAAC ext field at $z = 8.76$ (Cuby et al. 2007). No sources were found.

Table 1. Survey parameters taken from Shimasaku et al. (2006)^a, Rhoads et al. (2004)^b, Taniguchi et al. (2005)^c, Kashikawa et al. (2006)^d, Iye et al. (2006)^e, Willis & Courbin (2005)^f, Willis et al. (2006)^g, and Cuby et al. (2007)^h.

Name of survey	Telescope	Central λ (\AA)	Bandwidth (\AA)	Central z	Redshift Range	Area (arcmin^2)	Ref
Subaru Deep Field	Subaru	8150	120	5.7	5.64 – 5.76	725	a
LALA	Mayall	9182	84	6.55	6.516 – 6.586	1296	b
Subaru Deep Field	Subaru	9196	132	6.56	6.508 – 6.617	876	c, d
Subaru Deep Field	Subaru	9755	200	7.025	6.94 – 7.11	876	e
ZEN	VLT	11900	89.5	8.76	8.725 – 8.798	4	f, g
ISAAC ext	VLT	11900	89.5	8.76	8.725 – 8.798	31	h

Table 2. Best-fitting Schechter parameters from Kashikawa et al. (2006). These data are plotted in Figure 2.

Redshift	α	$\log_{10}(L^*/h_{70}^{-2} \text{ erg s}^{-1})$	$\log_{10}(\phi^*/h_{70}^3 \text{ Mpc}^{-3})$
6.5	-2.0	42.74	-3.14
	-1.5	42.60	-2.88
	-1.0	42.48	-2.74
5.7	-2.0	43.30	-3.96
	-1.5	43.04	-3.44
	-1.0	42.84	-3.14

(See Fig. 2.) As the mass-to-light ratio increases, the star formation is spread out over a longer period of time. Therefore, the galaxies are dimmer because less stars are shining at any given time.

We find that the Subaru data at $z = 5.7$ and $z = 6.56$ are consistent with no evolution of properties of Ly α emitters or the IGM opacity. The evolution in the number density of Ly α emitters can be explained solely by the evolution of the halo mass function. These points have been made already by Malhotra & Rhoads (2004); Dijkstra et al. (2007); McQuinn et al. (2006). At $z = 5.7$ we find that $M_h/L_{band} = 95 - 120$ fits the Subaru data from Shimasaku et al. (2006), with lower values favored near the flux density limit, where it is harder to correct for sample completeness. At $z = 6.56$ a slightly (20%) smaller value, $M_h/L_{band} = 85 - 100$, fits the Subaru data from Kashikawa et al. (2006). (These are fit for the values of L_{band} below $10^{43} \text{ erg s}^{-1}$ to the flux density limit, for most of the observational data fall between these limits.)

The high value of $M_h/L_{band} = 95 - 120$ at $z = 5.7$ seems to fall outside the Poisson error at $z = 6.56$ near the flux density limit, although at higher fluxes its statistical significance is more questionable. If we take this $\sim 20\%$ decrease in M_h/L_{band} seriously, an interesting conclusion may be drawn. First of all, the decrease in M_h/L_{band} from $z = 5.7$ to $z = 6.56$ is qualitatively inconsistent with the evolution of neutral fraction in the IGM. If the IGM was more neutral (i.e., less ionized) in the past, we should observe the increase in M_h/L_{band} at higher z . The evolution in M_h/L_{band} may be even more significant than it looks now, once the redshift effect is taken into account. Since the survey at $z = 6.56$ collects less photons than that at $z = 5.7$ for a given bandwidth of the instrument, one must take into account the bandwidth properly before making a quantitative comparison between M_h/L_{band} from two different redshifts. We shall perform this analysis more carefully in section 4.4.

Our finding may suggest that (i) Ly α emitters at $z = 6.56$ are brighter intrinsically than those at $z = 5.7$, or (ii) the intrinsic luminosity is the same, but more Ly α photons escaped from galaxies at $z = 6.56$ than from $z = 5.7$. (The absorption in the IGM was kept the same.) The possibility (ii) is quite plausible, if dust content of galaxies at $z = 6.56$ is less than that at $z = 5.7$. How much less requires a more careful analysis, which we shall give in section 4.4.

In order to put better constraints on the bright end of the luminosity function, a larger survey is needed. The brightest Ly α emitter detected at $z=5.7$ had a narrow band magnitude of 23.41 and the brightest at $z=6.56$ had a narrow band magnitude of 24.13. To detect brighter Ly α emitters, a larger survey would be needed that could find the rare, high density peaks of the mass function. In order to detect 10 galaxies above a magnitude of 23.41 at $z=5.7$, the survey would need to be at least 6.34 degree² if we assume M_h/L_{band} of 120, and at least 3.13 degree² if we assume a M_h/L_{band} of 95. For the Subaru field at $z=6.56$, to detect 10 galaxies with a narrow band magnitude of 24.13 or higher, the area of the survey would have to be 3.6 degree² if we assume a M_h/L_{band} of 100 and 2.2 degree² if we assume a M_h/L_{band} of 85.

The LALA data (Rhoads et al. 2004) also probe a very similar redshift, $z = 6.55$. Since only one galaxy was found from LALA, the Poisson error is large. Nevertheless, the LALA data give us an important cross-check of the results obtained from the Subaru field at the same redshift. We find that $M_h/L_{band} \sim 160$ explains LALA's detection of one galaxy at $z = 6.55$. When we compare the LALA and Subaru counts, we must take into account the different bandwidths of these surveys. The LALA's bandwidth is about 60% narrower than Subaru's (Table 1), and thus the constraint from the LALA data would correspond to $M_h/L_{band} \sim 100$ for the Subaru data. We thus conclude that the constraints from the Subaru and LALA fields at $z = 6.55$ are comfortably

consistent with each other. A more thorough comparison will be given in section 4.3.

At $z = 7.0$ Iye et al. (2006) discovered one Ly α emitter in the Subaru field that was confirmed spectroscopically. While the Poisson error is large, we find that $M_h/L_{band} \sim 100$ explains Subaru’s detection of one galaxy at $z = 7.0$. This number is remarkably similar to what we have found from the Subaru fields at $z = 5.7$ and 6.56 as well as from the LALA field at $z = 6.55$.

At $z = 8.76$ the searches performed in the ISAAC/VLT fields yielded null results. We therefore place lower limits to $M_h/L_{band} > 7$ and 3 from the ZEN and ISAAC ext, respectively. The weaker constraint from the latter is due to a brighter flux density limit. These lower limits are consistent with properties of Ly α emitters as constrained by the other searches at $z \leq 7$.

In order to improve upon these results, how large of a survey would be needed? In order for 10 galaxies above the flux density limit to be seen in the Subaru ($z=7.025$) and the LALA fields, the survey area would need to be increased to 2.5 degree² and 3.4 degree² respectively. If we assume that the mass to light ratio and α_{esc} is the same at $z=8.76$ than it is at $z=7.025$, the survey area of the ZEN and ISAAC ext fields would need to be increased to 24.8 and 1.69×10^5 degree² respectively. The area needed for the ISAAC ext field is larger than the entire sky, so it becomes apparent that an adjustment to the bandwidth or flux density detection limit is necessary to make finding a Ly α emitter more feasible.

In summary, properties of Ly α emitters and the IGM opacity have not evolved very much between $z = 5.7$ and 7. The lack of detection at $z = 8.76$ is also consistent with no evolution, although it does not provide a significant constraint yet.

4.2 Finding a mass-to-“bolometric light” ratio

Our analysis so far has been relatively model-independent. We have extracted the only free parameter, M_h/L_{band} , from various narrow-band searches of Ly α emitters.

Here, M_h/L_{band} only describes the light observed over the narrow band (the luminosity within the bandwidth, L_{band} , not the bolometric luminosity, L_{bol}). To proceed further and understand physical properties of Ly α emitters better, however, we must relate M_h/L_{band} to the mass-to-“bolometric light” ratio, M_h/L_{bol} , taking into account stellar populations as well as differences in the bandwidths.

In order to get the actual mass to light ratio, the spectra of a stellar population of galaxies must be modeled and integrated first over all frequencies and then compared to the light that is observed in the narrow band. The fraction of Ly α photons that survived, α_{esc} , also needs to be taken into account.

As a result, each data-set yields a constraint on $(M_h/L_{bol})\alpha_{esc}^{-1}$ as a function of assumed stellar populations.

When the duty cycle is less than unity, the constraint should be interpreted as $(M_h/L_{bol})(\alpha_{esc}\epsilon^{1/\gamma})^{-1}$, where $\gamma \sim 2$ is a local slope of the cumulative luminosity function, $N(>L) \propto L^{-\gamma}$, to which the current data are sensitive.

The spectra of a population of stars depend on the stellar mass spectrum and metallicity of stars. We shall use a va-

riety of mass functions paired with metallicities: (a) Salpeter (Salpeter 1955):

$$f(m) \propto m^{-2.35}, \quad (7)$$

(b) Larson (Larson 1998):

$$f(m) \propto m^{-1} \left(1 + \frac{m}{m_c}\right)^{-1.35}, \quad (8)$$

which matches Salpeter’s in the limit of $m_c \rightarrow 0$. One can explore a variety of models by changing one parameter, m_c .

(c) A top-heavy spectrum:

$$f(m) \propto \begin{cases} m^{-1}, & 100 < m < 500 M_\odot \\ 0, & \text{otherwise,} \end{cases} \quad (9)$$

which might be possible for the primordial metal-free stars (Bromm & Larson 2004). (Note that $mf(m)$ is flat for $100 < m < 500 M_\odot$.) The normalizations are given by

$$\int_{m_1}^{m_2} dm f(m) = 1, \quad (10)$$

with m_1 and m_2 being the mass limits that the mass function is integrated over. We also consider a delta function mass spectrum, with populations consisting of only 300 M_\odot stars.

The synthetic spectrum emerging from a galaxy with a given population of stars is the result of a variety of radiation processes. Some of the light from the star is converted by the nebula into the Ly α line, free-free, free-bound, and two-photon emission.

We use analytical formulae for these spectra given in section 2 of Fernandez & Komatsu (2006), paired with a line profile of Ly α emission from Loeb & Rybicki (1999); Santos et al. (2002). These formulae are fully analytic and therefore it is easy to adjust various parameters. We have checked that our predicted luminosities agree well with those produced from the numerical code, CLOUDY.

Care must be taken when one computes the profile of Ly α line. The width of the line profile we adopt here is likely too broad, as this profile assumes that the IGM around a source is completely neutral. The other extreme case, a delta function profile at 10.2 eV, increases the inferred M_h/L_{bol} by a factor of at most a few. We study this issue further in Appendix A.

We explore three metallicities: what we refer to as Population III ($Z = 0$), Population II ($Z = 1/50 Z_\odot$), and Population I ($Z = 1 Z_\odot$). For convenience we have fit the theoretical stellar data for bolometric luminosity, stellar temperature, lifetime, and number of ionizing photons. The fitting functions, given in Table 3 and plotted in Fig. 3, have been obtained by fitting stellar models provided by the papers given in the third column of Table 3.

In Fig. 4, we show the luminosity integrated over a mass spectrum divided by the average stellar mass:

$$\frac{\int_{m_1}^{m_2} L_{\nu,i} f(m) dm}{\int_{m_1}^{m_2} m f(m) dm} \quad (11)$$

for each component i , which includes stellar black-body, Ly α , free-free, free-bound, and two-photon.

Now we are in a position to calculate a conversion factor from L_{band} to L_{bol} :

$$\frac{L_{band}}{L_{bol}} = \frac{\int_0^{\nu_{max}} d\nu \sum_i \int_{m_1}^{m_2} L_{\nu,i} f(m) dm}{\int_0^\infty d\nu \sum_i \int_{m_1}^{m_2} L_{\nu,i} f(m) dm}, \quad (12)$$

Table 3. Fitting functions for the number of hydrogen ionizing photons per second, $Q(H)$, stellar temperature of the star, T_{eff} , bolometric luminosity of the star, L_{bol}^* , and stellar lifetime, τ_* , for varying metallicities. These were obtained from stellar models from Marigo et al. (2001)^a, Lejeune & Schaerer (2001)^b, and Schaerer (2002)^c, or the fitting functions from Schaerer (2002)^d. Note that $y \equiv \log(M_*/M_\odot)$, and log is a logarithm of base 10.

$Z = 0$	Fitting Function	Ref.
$\log[Q(H)/s^{-1}]$	$43.61 + 4.90y - 0.83y^2$ for $9 \leq M_* \leq 500M_\odot$	d
	$39.29 + 8.55y$ for $5 \leq M_* < 9M_\odot$	d
	0 for $M_* < 5$	
$\log[T_{eff}/K]$	$3.64 + 1.50y - 0.556y^2 + 0.070y^3$ for $M_* \geq 10M_\odot$	c
	$3.87 + 0.937y - 0.156y^2$ for $M_* < 10M_\odot$	a
$\log[L_{bol}^*/L_\odot]$	$0.457 + 3.90y - 0.530y^2$ for $M_* \geq 10M_\odot$	c
	$0.219 + 4.51y - 0.923y^2$ for $M_* < 10M_\odot$	a
$\log[\tau_*/year]$	$9.79 - 3.76y + 1.41y^2 - 0.186y^3$ for $M_* \geq 10M_\odot$	c
	$9.80 - 3.52y + 1.18y^2 - 0.164y^3$ for $M_* < 10M_\odot$	a
<hr/>		
$Z = 1/50 Z_\odot$		
$\log[Q(H)/s^{-1}]$	$27.80 + 30.68y - 14.80y^2 + 2.50y^3$ for $M_* \geq 5$	d
	0 for $M_* < 5$	
$\log[T_{eff}/K]$	$3.86 + 0.898y - 0.299y^2 + 0.0399y^3$	b
$\log[L_{bol}^*/L_\odot]$	$0.175 + 4.26y - 0.652y^2$	b
$\log[\tau_*/year]$	$9.82 - 3.13y + 0.743y^2$	b
<hr/>		
$Z = 1 Z_\odot$		
$\log[Q(H)/s^{-1}]$	$27.89 + 27.75y - 11.87y^2 + 1.73y^3$ for $M_* \geq 5$	d
	0 for $M_* < 5$	
$\log[T_{eff}/K]$	$3.74 + 0.826y - 0.166y^2$	b
$\log[L_{bol}^*/L_\odot]$	$-0.148 + 4.70y - 0.781y^2$	b
$\log[\tau_*/year]$	$10.08 - 3.47y + 0.774y^2 + 0.0327y^3$	b

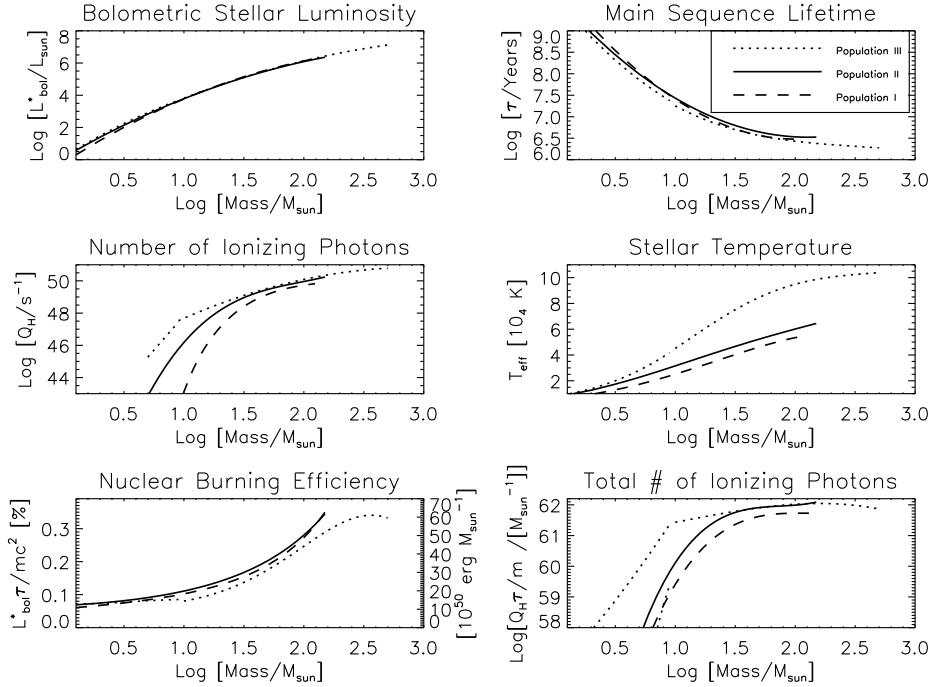


Figure 3. Fitting functions for the theoretical stellar data for the stellar bolometric luminosity, L_{bol}^* , lifetime, τ_* , the number of hydrogen ionizing photons per second, $Q(H)$, and the stellar temperature, T_{eff} , for varying metallicities: $Z = 0$ (Population III), $Z = 1/50 Z_\odot$ (Population II), and $Z = 1 Z_\odot$ (Population I). The fitting formulae are given in Table 3. In addition, the nuclear burning efficiency (the total radiation energy produced over the stellar lifetime divided by the rest mass energy, M_*c^2), and the total number of ionizing photons over the star's lifetime are plotted.

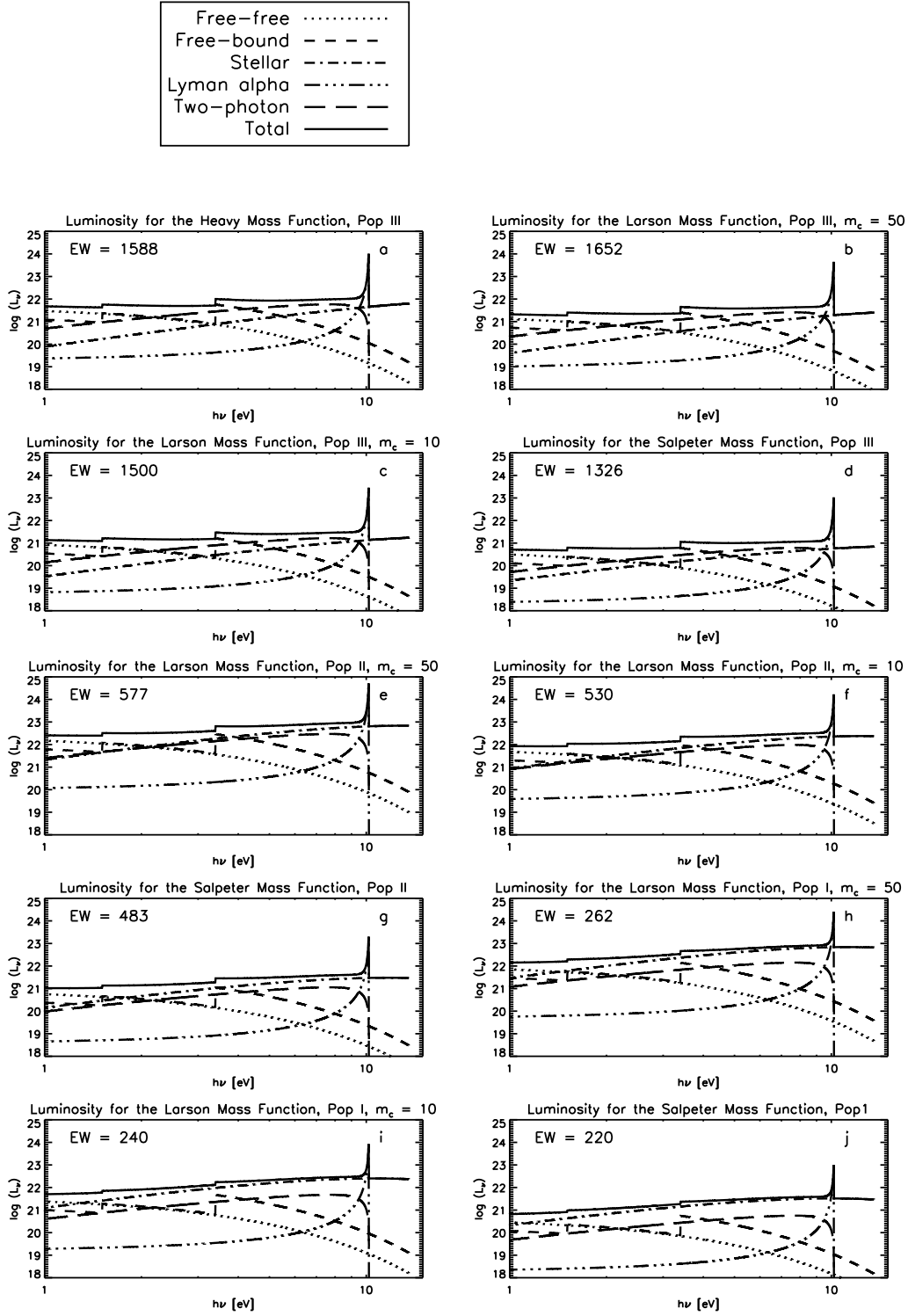


Figure 4. Rest-frame spectra of galaxies with various populations of stars integrated over a mass spectrum. The vertical axis is in units of $\text{erg s}^{-1} \text{Hz}^{-1} M_{\odot}^{-1}$. The solid lines show the total spectra, while the dotted, short dashed, dot-dashed, dot-dot-dot-dashed, and long dashed lines show the free-free, free-bound, stellar, Ly α , and two-photon emission, respectively. We have adopted a Ly α profile from Loeb & Rybicki (1999); Santos et al. (2002). (For further discussion of the profile, see Appendix A.) We show the luminosity averaged over various mass spectra, given in section 4, divided by the mean stellar mass. The spectra are computed for a galaxy at $z = 7.025$, although the redshift affects the shape of the Ly α line profile only. The equivalent width (EW) of the Ly α line before extinction or scattering is also given. The EW has been computed from $\text{EW} = (\text{Total flux in Ly}\alpha) / (\text{Continuum flux at } 1216 \text{ \AA})$.

Table 4. Ratio of luminosity observed within the bandwidths of Subaru ($L_{Sub,z=5.7}$, Shimasaku et al. 2006; $L_{Sub,z=6.56}$, Taniguchi et al. 2005; Kashikawa et al. 2006; $L_{Sub,z=7}$, Iye et al. 2006), LALA (L_{LALA} , Rhoads et al. 2004), and ZEN and ISAAC ext (L_{ISAAC} , Willis & Courbin 2005; Willis et al. 2006; Cuby et al. 2007) in comparison to the bolometric luminosity, L_{bol} , for a variety of mass spectra and metallicities, in the absence of absorption or extinction of Ly α . The ratio is nearly independent of stellar mass spectra, while it drops as the metallicity of stars increases.

Metallicity (Z_{\odot})	$f(m)$	$m_1, m_2(M_{\odot})$	$\frac{L_{Sub,z=5.7}}{L_{bol}}$	$\frac{L_{LALA}}{L_{bol}}$	$\frac{L_{Sub,z=6.56}}{L_{bol}}$	$\frac{L_{Sub,z=7}}{L_{bol}}$	$\frac{L_{ISAAC}}{L_{bol}}$
0	$300M_{\odot}$ δ -function	–	0.312	0.209	0.263	0.297	0.120
0	Heavy	100, 500	0.311	0.209	0.262	0.297	0.120
0	Larson, $m_c = 50M_{\odot}$	0.8, 150	0.313	0.210	0.264	0.299	0.120
0	Larson, $m_c = 10M_{\odot}$	0.8, 150	0.305	0.205	0.257	0.291	0.117
0	Salpeter	0.8, 150	0.293	0.197	0.247	0.280	0.113
1/50	Larson, $m_c = 50M_{\odot}$	0.8, 150	0.219	0.146	0.185	0.210	0.0843
1/50	Larson, $m_c = 10M_{\odot}$	0.8, 150	0.209	0.139	0.176	0.201	0.0806
1/50	Salpeter	0.8, 150	0.198	0.131	0.167	0.190	0.0761
1	Larson, $m_c = 50M_{\odot}$	0.8, 120	0.143	0.0945	0.121	0.138	0.0555
1	Larson, $m_c = 10M_{\odot}$	0.8, 120	0.134	0.0881	0.113	0.130	0.0519
1	Salpeter	0.8, 120	0.124	0.0813	0.105	0.120	0.0480

where $\nu_{max} = \nu_{2,obs}(1+z)$ and $\nu_{min} = \nu_{1,obs}(1+z)$ are the limiting frequencies of instruments in the rest frame of the galaxies (again assuming a rectangular bandpass), $L_{\nu,i}$ is the luminosity of each component, and m_2 and m_1 are the mass limits of the stellar mass spectrum, $f(m)$.

In Table 4 we show L_{band}/L_{bol} for the various surveys. We find that L_{band}/L_{bol} is fairly constant over different mass spectra, but depends mainly on metallicity. Metal-free stars sustain higher temperatures as they undergo nuclear burning through the p-p chain. Because of this, their stellar spectrum is harder than stars with metals (see panels a-d in Fig. 4). Therefore they emit more ionizing photons that can be converted by the surrounding nebula into the Ly α line. As the metallicity increases (panels e-j), the stellar temperature decreases, the stellar spectrum softens, the ionizing photon flux decreases, and thus the Ly α line is depleted for a given stellar mass. As a result, one obtains a lower L_{band}/L_{bol} for a higher metallicity.

Now, calculating the mass-to-bolometric light ratio of galaxies is simple: multiply the mass-to-observed light ratio (M_h/L_{band}) by the ratio of observed to bolometric luminosity given in Table 4.

This is, however, not the end of story. Not all Ly α photons would escape from galaxies due to dust extinction, or from the IGM due to resonant scattering. We are unable to distinguish these two effects; thus, we parametrize a combined effect by a single parameter, α_{esc} , a survival fraction of Ly α photons.

4.3 Results

The outcome of our analysis is a mass-to-bolometric light ratio divided by a Ly α survival fraction and the effect of duty cycle, $(M_h/L_{bol})(\alpha_{esc}\epsilon^{1/\gamma})^{-1}$, where L_{bol} is the *intrinsic* luminosity of galaxies before absorption or extinction of Ly α photons. We tabulate this quantity inferred from various narrow-band searches in Table 5, which is the main result of this paper.

Since the effect of bandwidths has been taken into account properly, these constraints can be compared with each other on equal footing. Let us analyze the results in Table

5. As noted in the previous section, the Ly α line diminishes in strength and $(M_h/L_{bol})(\alpha_{esc}\epsilon^{1/\gamma})^{-1}$ drops as metallicity increases. A variation due to different stellar mass spectra is negligible.

The values of $(M_h/L_{bol})(\alpha_{esc}\epsilon^{1/\gamma})^{-1}$ inferred from the current data processed through our simple model are rather reasonable: for all cases where at least one source is found per field, the inferred $(M_h/L_{bol})(\alpha_{esc}\epsilon^{1/\gamma})^{-1}$ falls between 9 and 38, the low and high values being for the solar and zero metallicity, respectively. Consistency across redshifts ($z = 5.7, 6.5,$ and 7.0) as well as across different observations is striking.

We conclude from these results that the Ly α emitters detected in these narrow-band surveys are either normal galaxy populations with $M_h/L_{bol} \sim 10$ and having a fair fraction of Ly α photons escape, $\alpha_{esc}\epsilon^{1/\gamma} \sim 0.5 - 1$, or starburst galaxies with $M_h/L_{bol} \sim 0.1 - 1$ and a smaller fraction of the Ly α photons escaped from the galaxies themselves *and* the surrounding IGM, $\alpha_{esc}\epsilon^{1/\gamma} \sim 0.01 - 0.05$. Note that the degeneracy still allows for a possibility of having a significant survival fraction from these starburst populations, e.g., $\alpha_{esc} \sim 0.5$, if $\epsilon^{1/\gamma} \sim 0.1$ (or $\epsilon \sim 0.01$ and $\gamma \sim 2$).

It is clear that α_{esc} , ϵ , and M_h/L_{bol} are completely degenerate: we can only constrain the product of these three properties, not the individual properties.

The ratio of the Ly α flux to the continuum flux helps to lift this degeneracy partially. The observed equivalent width (EW) of Ly α emitters is on the order of 100 Å or larger (e.g., Kashikawa et al. 2006). In Figure 4 we show the predicted EW,

$$EW = \frac{\text{Total Flux in Ly}\alpha}{\text{Continuum Flux at } 1216 \text{ \AA}}, \quad (13)$$

Using the zero-age main sequence values for the luminosity (given in Table 3), we obtain equivalent widths of 1300–1700 for $Z = 0$, 480 – 580 for $Z = 1/50 Z_{\odot}$, and 220 – 260 for $Z = 1 Z_{\odot}$. Therefore, a low survival fraction, $\alpha_{esc} \sim 0.1$, is required for low metallicity populations, while a high $\alpha_{esc} \sim 0.5$ is required for high metallicity ones, in order to fit the observed EW. However, as the age of stars within the galaxy increase, the fraction of ionizing photons to non-ionizing pho-

Table 5. The mass (total halo mass) to light (bolometric luminosity) ratio times $1/(\alpha_{esc} \epsilon^{1/\gamma})$. The luminosity refers to the intrinsic luminosity before absorption or extinction of Ly α photons. For each metallicity of stellar populations ($Z = 0$, $Z = 1/50 Z_{\odot}$, and $Z = 1 Z_{\odot}$) a range of values represent a range of stellar mass spectra. For the observational data we used $M_h/L_{band} = 95 - 120$ and $85 - 100$ for the Subaru fields at $z = 5.7$ and 6.56 , respectively, whereas we used $M_h/L_{band} \sim 160$ and ~ 100 for the LALA field at $z = 6.55$ and the Subaru field at $z = 7.025$. The latter values are much more uncertain than the former ones due to a large Poisson error, as only one Ly α emitter was found in each of the latter fields. For the ZEN and ISAAC fields only lower limits are given, as no sources were found in these fields. Note that $\gamma \sim 2$ for the surveys listed here.

Field	Redshift	$\frac{M_h}{L_{bol}} \frac{1}{\alpha_{esc} \epsilon^{1/\gamma}}$ ($Z = 0$)	$\frac{M_h}{L_{bol}} \frac{1}{\alpha_{esc} \epsilon^{1/\gamma}}$ ($Z = 1/50 Z_{\odot}$)	$\frac{M_h}{L_{bol}} \frac{1}{\alpha_{esc} \epsilon^{1/\gamma}}$ ($Z = 1 Z_{\odot}$)
Subaru	5.7	28 – 38	19 – 26	12 – 17
LALA	6.55	$\sim 32 - 34$	$\sim 21 - 23$	$\sim 13 - 15$
Subaru	6.56	21 – 26	14 – 19	8.9 – 12
Subaru	7.025	$\sim 28 - 30$	$\sim 19 - 21$	$\sim 12 - 14$
ZEN	8.76	$> 0.79 - 0.84$	$> 0.53 - 0.59$	$> 0.34 - 0.39$
ISAAC ext	8.76	$> 0.34 - 0.36$	$> 0.23 - 0.25$	$> 0.14 - 0.17$

tons decrease, and thus less photons are converted into Ly α photons. Therefore, the equivalent width may decrease with time - depending on the age of the galaxy and the rate of star formation. (Charlot & Fall 1993; Leitherer et al. 1999; Kudritzki et al. 2000; Malhotra & Rhoads 2002; Schaerer 2003)

Assuming the zero-age main sequence luminosity of the stars, there are two solutions left for $\epsilon \sim 1$: (i) Ly α emitters at $z \geq 5.7$ are normal populations with $Z > 1/50 Z_{\odot}$ and $\alpha_{esc} > 0.5$, or (ii) they are starburst populations with $Z < 1/50 Z_{\odot}$ and $\alpha_{esc} < 0.1$. As stars age, the EW of the population will also decrease, allowing for larger values of α_{esc} for a $Z < 1/50 Z_{\odot}$ population. For $\epsilon < 1$ other solutions are still allowed.

Having the Ly α line be diminished in flux by about an order of magnitude is not a surprising effect. Both the IGM and galaxies themselves are expected to scatter or absorb Ly α photons efficiently. Dijkstra et al. (2007) claim that the asymmetry in Ly α lines that has been seen in the current data already suggests that the IGM only transmitted 10 – 30% of the Ly α flux. Several authors model the effect of dust (Hansen & Oh 2006; Verhamme et al. 2006) and neutral hydrogen (Laursen & Sommer-Larsen 2007) within galaxies on Ly α photons, and find that even a small amount of dust can easily absorb Ly α photons, and the resulting line profiles may be complex due to a structure in the distribution of dust and outflows. In addition, high opacity near the line centre decreases the flux at the centre of the line. However, if the medium is clumpy, the ratio of Ly α to continuum photons might actually be increased (Neufeld 1991; Hansen & Oh 2006). McQuinn et al. (2006) also study the effect of neutral hydrogen on the Ly α line using cosmological simulations. Once the universe is almost totally reionized, there will not be much suppression of the Ly α line, but before then, Ly α luminosity might be able to help probe the size of HII bubbles – the larger the bubble, the less suppression of the Ly α line (Haiman & Cen 2005).

The physics of this problem is complex; however, our results are consistent with a depletion of the Ly α flux if indeed these Ly α emitters are starburst galaxies with $M_h/L_{bol} \sim 0.1 - 1$.

4.4 Interesting features

Is there any “anomaly”? Let us focus on the Subaru fields at $z = 5.7$ and 6.56 , as these are the most accurate data-sets. We observe nearly 20–30% decrease in $(M_h/L_{bol})(\alpha_{esc}\epsilon^{1/\gamma})^{-1}$ from $z = 5.7$ to $z = 6.56$. We saw this trend in the preliminary analysis based upon M_h/L_{band} in section 4.1. After a more careful analysis we still observe the same trend.

Although subtle, if this is indeed a real effect, what would be the implication? This effect *cannot* be explained by having a smaller α_{esc} (hence a larger opacity for Ly α photons) at higher z . Therefore, it is inconsistent with neutral fraction in the IGM around sources being higher at higher z . On the contrary, one needs to have a larger α_{esc} – hence a smaller opacity for Ly α photons – at higher z , perhaps due to less dust content (Haiman & Spaans 1999). An alternative possibility is that M_h/L_{bol} was lower in the past, i.e., the Ly α emitters were intrinsically brighter at higher z , perhaps due to a more intense starburst. Such a burst would create a large HII bubble around the source, which also helps to increase α_{esc} by suppressing the IGM opacity. It therefore seems easy to explain the 20–30% decrease in $(M_h/L_{bol})(\alpha_{esc}\epsilon^{1/\gamma})^{-1}$ from $z = 5.7$ to 6.5 . A similar trend has also been pointed out by Stark et al. (2007).

As we show in Appendix A, the magnitude of this effect is reduced to 10–20% if we assume that a line profile of Ly α photons is a delta function at 10.2 eV.

Another interesting feature in Table 5 is that $(M_h/L_{bol})(\alpha_{esc}\epsilon^{1/\gamma})^{-1}$ at $z = 6.56$ for $Z = 0$ agrees with that at $z = 5.7$ for $Z = 1/50 Z_{\odot}$, and $(M_h/L_{bol})(\alpha_{esc}\epsilon^{1/\gamma})^{-1}$ at $z = 6.56$ for $Z = 1/50 Z_{\odot}$ agrees with that at $z = 5.7$ for $Z = 1 Z_{\odot}$. While it seems a mere numerical coincidence, it might also be suggestive of the metallicity evolution in Ly α emitters.

5 COMPARISON WITH PREVIOUS WORK

A halo mass function as a tool for calculating the luminosity function of Ly α emitters is not a new idea (e.g., Haiman & Spaans 1999; Haiman et al. 2000).

Novelty of our approach is the use of the mass-to-light ratio as a fundamental parameter, which has a few advantages. In this section we make this point clear by comparing our results with recent work on a similar subject.

In addition, our analysis is new in that we have explored various assumptions about metallicity and stellar mass spectra of Ly α emitters.

5.1 Dijkstra et al. (2006)

Dijkstra et al. (2006) computed $N(> F)$ by integrating the halo mass function over mass above a certain flux density, F . In order to relate the host halo mass to the observed luminosity, L_α ,¹ they used

$$\frac{M_h}{L_\alpha} = 0.128 \times \frac{t_{sys}/(100 \text{ Myr})}{\frac{\Omega_b}{\Omega_m} \eta \alpha_{esc}}, \quad (14)$$

which is their equation (2) in our notation. (Note that in our notation M/L is always measured in units of M_\odot/L_\odot^{-1} .) Here, η is the fraction of baryon mass converted into stars, $t_{sys} = \epsilon t_{hub}$ is the duration of a starburst, t_{hub} is the Hubble time, and ϵ is the duty cycle.

In our approach M_h/L_α is the only free parameter, and the effect of ϵ is included using the degeneracy line, $(M_h/L_\alpha)\epsilon^{-1/\gamma} = \text{constant}$. Their approach was to divide M_h/L_α up further by introducing two free parameters, ϵ and $\eta\alpha_{esc}$, and constrain these parameters simultaneously. However, it is difficult to extract more than M_h/L_α from the observed luminosity function. Figure 1 of Dijkstra et al. (2006) also shows that ϵ and $\eta\alpha_{esc}$ are strongly degenerate. In our opinion the current data do not allow for two free parameters to be constrained well. In addition, the use of M_h/L_α as a parameter avoids the need to specify the duration of a starburst or the fraction of baryon mass converted into stars.

They found that α_{esc} at $z = 5.7$ inferred from Shimasaku et al. (2006) and α_{esc} at $z = 6.5$ inferred from Taniguchi et al. (2005); Kashikawa et al. (2006) are about the same, the ratio of the two being $\alpha_{esc,57}/\alpha_{esc,65} \sim 0.8 - 1.5$ for a prior on ϵ of $\epsilon = 0.5 - 0.03$. We would find $\alpha_{esc,57}/\alpha_{esc,65} \sim 0.7 - 0.8$ (see Table 5), if we assumed that the intrinsic properties of Ly α emitters did not change between these redshifts. The other values of α_{esc} are permitted when we vary the intrinsic mass-to-light, M_h/L_{bol} , with $(M_h/L_{bol})(\alpha_{esc}\epsilon^{1/\gamma})^{-1}$ held fixed. This is essentially equivalent to their varying ϵ along the degeneracy line.

When an additional constraint from the luminosity function of UV continuum was included in the analysis, they found that the constraints shifted slightly to $\alpha_{esc,57}/\alpha_{esc,65} \sim 1.1 - 1.8$. While we do not perform a joint analysis with the UV continuum luminosity function in this paper, we would expect a similar shift in the parameter constraint.

5.2 Salvaterra & Ferrara (2006)

Salvaterra & Ferrara (2006) used an stellar mass spectrum

of stars that is given by a delta function at $m_* = 300 M_\odot$, and related M_h to L_{band} as

$$\frac{M_h}{L_{band}} = \frac{300 M_\odot}{\int_{\nu_{min}}^{\nu_{max}} d\nu \sum_i L_{\nu,i}(300 M_\odot) \frac{\Omega_b}{\Omega_m} \eta}, \quad (15)$$

which can be obtained from their equation (3), combined with our equation (4). Their M_h/L_{band} is therefore equal to about 10 times² the mass-to-light of a metal-free star of $300 M_\odot$.

The lifetime of a starburst of their model galaxy is as short as the lifetime of stars, which is only 2 Myr. In other words, they assumed that these massive stars formed at once in a galaxy, so that the lifetime of starbursts was the shortest possible time, equal to the lifetime of the star. This creates a very short lived but extremely bright galaxy that could easily be detected with current observations.

The mass-to-bolometric light ratio of their model galaxy was $M_h/L_{bol} = 6.73 \times 10^{-4}$ and 1.35×10^{-3} for ‘‘H-cooling’’ and ‘‘H₂-cooling’’ haloes, respectively, assuming all Ly α photons escaped. (They used $\eta = 0.8$ and 0.4 for H-cooling and H₂-cooling haloes, respectively.) These extreme values allow them to predict that there should be thousands of galaxies seen in the NICMOS Ultra Deep Field, where only three or fewer were actually detected, and 400 to 700 in the ZEN field, where no sources were detected. They also reported that almost all of the Spitzer counts should be attributed to galaxies above $z \sim 8$.

Their conclusion is driven by their fixed value of M_h/L_{bol} , which seems rather low. Our formulation, which treats M_h/L_{band} as a free parameter, allows for dimmer galaxies by spreading out the star formation over a much longer period than the stellar lifetime. This allows us to obtain results that are consistent with observations. Note that their using a delta-function mass spectrum is not the source of discrepancy. We can still fit the observations with a reasonable M_h/L_{bol} for the same mass spectrum. The source of discrepancy is their assumption about an instantaneous starburst in 2 Myr.

They used these bright galaxies to fit the observed excess in the near infrared background. The main conclusion of Salvaterra & Ferrara (2006) is that the excess near infrared background cannot be mainly coming from high- z galaxies at $z \gtrsim 7$, as they do not see these extremely bright galaxies in the NICMOS UDF, ZEN, or Spitzer counts.

However, their argument does not rule out the high- z galaxies being the origin of the near infrared background. Using a simple argument based upon energy conservation, we have shown in the previous paper (Fernandez & Komatsu 2006) that the near infrared background measures only the total light integrated over time, and thus one can obtain the same amount of near infrared background by having either (i) extremely bright sources over an extremely short time period, such as those invoked by Salvaterra & Ferrara (2006), or (ii) much dimmer sources over a much longer time period. While Salvaterra & Ferrara (2006) have successfully shown that the first possibility is ruled out, they have not ruled out the second possibility yet.

¹ Their luminosity, L_α , is different from our L_{band} , as they ignored the line profile, continuum, and bandwidth of instruments.

² $\Omega_m/(\Omega_b\eta) \sim 10$.

5.3 Le Delliou et al. (2006)

Le Delliou et al. (2006) predict the luminosity functions of Ly α emitters at redshifts from $3 < z < 6.6$, using cosmological simulations coupled with a semi-analytical galaxy formation model.

Similar to ours and the other work, they assume that the escape fraction of Ly α photons are independent of halo mass, and find its value, $\alpha_{esc} = 0.02$, by fitting the observed luminosity function of Ly α emitters at $z \sim 3$. (See Kobayashi et al. 2007, for a criticism on this assumption.)

Since the halo mass function is also an essential ingredient in the semi-analytical galaxy formation model, and they make the same assumption about the escape fraction of Ly α photons, we expect our predictions and theirs to agree well for the same set of parameters. We find that we can fit the bright-end of their predicted luminosity functions (their Fig. 1 for $z = 7$) with a population of starburst galaxies, $M_h/L_{bol} \sim 1$, which is a very reasonable result.

We believe that our simple model captures the basic physics that goes into their model, which is more sophisticated and complex.

At a fainter end, however, their luminosity function flattens out and our calculations always over-predict the number of sources. This is likely due to our assumption about a constant mass-to-light ratio. It is expected that this assumption breaks down once a large mass range is included in the analysis. The most economical way to improve our model is to introduce a second free parameter, a slope of mass-to-light, such that $L \propto M^\beta$, for instance. As the observations improve in the future, a two-parameter model such as this should be used.

6 CONCLUSIONS

A simple model based upon the halo mass function coupled with a constant mass-to-light ratio fits the luminosity functions measured and constrained by the current generation of narrow-band Ly α surveys from $5.7 \leq z \leq 8.8$. We have explored various metallicities and stellar mass spectra.

The inferred mass-to-light ratios are consistent with no evolution in the properties of Ly α emitters or opacity in the IGM from $5.7 \leq z \leq 7$. Therefore, the current data of the luminosity functions do not provide evidence for the end of reionization. The data at $z = 8.8$ do not yield a significant constraint yet.

These mass-to-light ratios suggest that the Ly α emitters discovered in the current surveys are either starburst galaxies with only a smaller fraction of Ly α photons escaped from galaxies themselves and the IGM, $\alpha_{esc}\epsilon^{1/\gamma} \sim 0.01 - 0.05$, or normal populations with a fair fraction of Ly α photons escaped, $\alpha_{esc}\epsilon^{1/\gamma} \sim 0.5 - 1$. The luminosity function alone cannot distinguish between these two possibilities.

For the duty cycle of order unity, $\epsilon \sim 1$, the observed equivalent width of Ly α line indicates that starburst populations are consistent with low metallicity populations with $Z < 1/50 Z_\odot$, while normal populations are consistent with high metallicity populations. The other solutions are still allowed for $\epsilon < 1$. Note that a recent study of the SED of Ly α emitters by Nilsson et al. (2007) shows that the Ly α emitters at $z = 3.15$ are consistent with a very low metallicity population, $Z = 1/200 Z_\odot$.

To constrain the properties of Ly α emitters further, one should use asymmetric absorption features of the measured Ly α line profiles to distinguish between them (Miralda-Escude 1998; Miralda-Escude & Rees 1998; Haiman 2002; Santos 2004; Tasitsiomi 2006). The best way to break degeneracy between ϵ and α_{esc} is to detect the deviation of the cumulative luminosity function from a pure power-law. In order to do this it is crucial to determine the bright end of luminosity function more accurately.

We disagree with the conclusion reached by Salvaterra & Ferrara (2006) that no detection of Ly α emitters at $z = 8.8$ excludes the excess near infrared background being produced by galaxies at $z > 7$. While they have excluded the excess background coming from extremely bright starburst galaxies with $M_h/L_{bol} \sim 10^{-3}$ and the lifetime of 2 Myr, their argument does not exclude another possibility that the excess background originates from galaxies with $M_h/L_{bol} \sim 0.1 - 1$ and the lifetime comparable to the age of the universe at $z > 7$. As the near infrared background measures only the total amount of light integrated over time, both scenarios result in the same amount of background light. As we have shown in this paper, the latter scenario is consistent with all the existing Ly α surveys from $5.7 \leq z \leq 8.8$.

There is a subtle hint that 20 – 30% more Ly α photons survived from $z = 6.5$ than from $z = 5.7$. A number of factors need to be checked carefully before this conclusion is taken seriously: the completeness correction and spectroscopic confirmation rate of the observed luminosity function, the shape of Ly α line profiles (which is however not quite enough to make the effect go away; see Appendix A), and accuracy of the evolution of the theoretical halo mass function in these redshifts. In addition, more elaborated theoretical models such as those described in Sec. 2.1 may be necessary to test reality of this effect, while it is interesting that the model with a duty cycle has also shown a similar trend (Stark et al. 2007).

Our method should provide a simple tool for interpreting the galaxy number count data in terms of the mass-to-light ratio. Or, for a given mass-to-light ratio as constrained by the existing data, it can also be used to predict the luminosity functions, and thus it helps to design future Ly α surveys such as a follow-up survey at $z = 7$ with Subaru, at $z = 8.8$ with VLT, and a new survey at even higher redshifts with the James Webb Space Telescope (see also Barton et al. 2004, for an alternative way of making forecasts).

ACKNOWLEDGMENTS

We would like to thank Kyungjin Ahn, Volker Bromm, Neal Evans, Juna Kollmeier, Paul Shapiro, Gregory Shields, and Chris Sneden for discussions, and Mark Dijkstra, Andrea Ferrara, and Tomonori Totani for their comments on the manuscript. We would also like to thank Robert Kurucz for his help on the compilation of the stellar data. E.R.F. acknowledges support from a Continuing Fellowship of the University of Texas at Austin. E.K. acknowledges support from an Alfred P. Sloan Fellowship.

APPENDIX A: ON THE PROFILE OF $\text{Ly}\alpha$ LINES

Throughout this paper we have adopted a theoretical line profile computed by Loeb & Rybicki (1999) and later fit by Santos et al. (2002) (their equation 15). This line profile is fairly broad (see dot-dot-dot-dashed lines in Figure 4). The physical origin of this broadening is a combination of the IGM scattering and cosmological redshift. Since their underlying assumption that the IGM around sources is neutral may not be always valid, a care must be taken when one uses their theoretical profiles. The broadening is reduced significantly when the IGM around sources is ionized.

The shape of the line profile affects our analysis through the bandwidths of instruments. Since we are dealing with narrow-band filters, instruments miss a large fraction of $\text{Ly}\alpha$ photons if a line profile is broader than their bandwidths. Therefore, if we assumed erroneously that the line profile was too broad, then the inferred M_h/L_{bol} would be too low.

In order to quantify a possible uncertainty regarding the shape of the line profile, we explore the extreme case where a line profile is a delta function at 10.2 eV. Since the instruments would not miss any $\text{Ly}\alpha$ photons, the luminosity within the band, L_{band} , would increase.

Table A1 shows that a delta-function line profile increases the luminosity within instrument's bandwidths substantially. For metal-free stars with a heavy mass spectrum, the luminosity increases by a factor of 2 for Subaru, a factor of 3 for LALA, and a factor of 5.5 for ISAAC.

In Table A2 we report the inferred $(M_h/L_{bol})(\alpha_{esc}\epsilon^{1/\gamma})^{-1}$ from assuming a delta function line profile. These values should be compared with those in Table 5. While there are changes in the inferred $(M_h/L_{bol})(\alpha_{esc}\epsilon^{1/\gamma})^{-1}$ at the level of a factor of a few, the main result from our analysis does not change: the $\text{Ly}\alpha$ emitters discovered in these surveys are either starburst galaxies with $\alpha_{esc}\epsilon^{1/\gamma} \sim 0.01 - 0.1$, or normal galaxies with $\alpha_{esc}\epsilon^{1/\gamma} \sim 0.5 - 1$.

On the other hand, a hint that $(M_h/L_{bol})(\alpha_{esc}\epsilon^{1/\gamma})^{-1}$ at $z = 6.56$ is smaller than that at $z = 5.7$ is now less significant: it's only a 10–20% effect, rather than a 20–30% effect.

REFERENCES

- Ajiki M. et al., 2003, AJ, 126, 2091
 Ajiki M. et al., 2004, PASJ, 56, 597
 Ajiki M., Mobasher B., Taniguchi Y., Shioya Y., Nagao T., Murayama T., Sasaki S. S., 2006, ApJ, 638, 596
 Barton E.J., Davé R., Smith J.-D.T., Papovich C., Hernquist L., Springel V., 2004, ApJ, 604, L1
 Becker R. H., 2001, AJ, 122, 2850
 Bromm V., Larson R. B., 2004, ARA&A, 42, 79
 Charlot S., Fall S.M., 1993, ApJ, 415, 580
 Cooray A., Milosavljevic, M., 2005, ApJ, 627, L89
 Cooray A., Yoshida N., 2004, MNRAS, 351, L71
 Cuby J.-G., Hibon P., Lidman C., Le Fevre O., Gilmozzi R., Moorwood A., van der Werf P., 2007, A&A, 461, 911
 Dijkstra M., Lidz A., Wyithe, J. S. B., 2007, MNRAS, 377, 1175
 Dijkstra M., Wyithe J. S. B., Haiman Z., 2006b, astro-ph/0611195
 Dwek E., Arendt R., Krennrich F., 2005, ApJ, 635,784
 Fan X. et al, 2000, AJ, 120, 1167
 Fan X. et al, 2001, AJ, 122, 2833
 Fan X., Narayanan V. K., Strauss M. A., White R. L., Becker R. H., Pentericci L. Rix H.-W., 2002, AJ, 123, 1247
 Fan X. et al, 2004, AJ, 128, 515
 Fernandez E., Komatsu E., 2006, ApJ, 646, 703
 Goto T., 2006, MNRAS, 371, 769
 Gunn J. E., Peterson B. A., 1965, ApJ, 142, 1633
 Haiman Z., 2002, ApJ, 576, L1
 Haiman Z., Cen R., 2005, ApJ, 623, 627
 Haiman Z., Spaans, M., 1999, ApJ, 518, 138
 Haiman Z., Spaans, M., Quataert, 2000, ApJ, 537, L5
 Hansen M., Oh S.P., 2006, MNRAS, 367,979
 Hu E.M., Cowie L.L., Capak P., McMahan R.G., Hayashino T., Komiyama Y., 2004, ApJ, 127, 563
 Hui L., Haiman Z., 2003, ApJ, 596, 9
 Iye M. et al., 2006, Nat, 443,186
 Kaplinghat M., Chu M., Haiman Z., Holder G. P., Knox L., Skordis C., 2003, ApJ, 583, 24
 Kashikawa N. et al. 2006, ApJ, 648, 7
 Kashlinsky A., Arendt R.G., Mather S.H., Moseley S.H., 2005, Nature, 438, 45
 Kashlinsky A., Arendt R.G., Mather S.H., Moseley S.H., 2007, ApJ, 654, L1
 Kobayashi M.A.R., Totani T., Nagashima M., 2007, arXiv:0705.4349
 Kogut A. et al., 2003, ApJs, 148, 161
 Kodaira K. et al., 2003, PASJ, 55, L17
 Kudritzki R.P. et al., 2000, ApJ, 536,19
 Kurk J.D., Cimatti A., di Serego Alighieri S., Vernet J., Daddi E., Ferrara A., Ciardi B., 2004, A&A, 422, L13
 Laursen P., Sommer-Larsen J., 2007, ApJ, 657,L69
 Larson R. B., 1999, MNRAS, 301, 569
 Le Delliou M., Lacey C.G., Baugh C.M., Morris S.L., 2006, MNRAS, 365, 712
 Leitherer C. et al., 1999, ApJ, 123, 3
 Lejeune T., Schaerer D., 2001, A&A, 336, 538L
 Loeb A., Rybicki G., 1999, ApJ, 524, L527
 Madau P., Silk J., 2005, MNRAS, 359, L37
 Maier C. et al., 2003, A&A, 402, 79
 Malhotra S., Rhoads J.E., 2002, ApJ, 565, L71
 Malhotra S., Rhoads J., 2004, ApJ, 617,L5
 Marigo P., Girardi L., Chiosi C., Wood P. R., 2001, A&A, 371,152
 Martin C.L., Sawicki M., 2004, ApJ, 603, 414
 McQuinn M., Lidz A., Zahn O., Suvendra D., Hernquist L., Zaldarriaga M., 2006, astro-ph/0610094
 Mii H., Totani T., 2005, ApJ, 628, 873
 Miralda-Escude J., 1998, ApJ, 501, 15
 Miralda-Escude J., Rees M.J., 1998, ApJ, 497, 21
 Mobasher B. et al., 2005, ApJ, 635, 832
 Murayama T. et al., 2007, astro-ph/0702458
 Neufeld D.A., 1991, ApJ, 370,L85
 Nilsson K.K. et al., 2007, arXiv:0706.1070
 Oh S.P., Furlanetto S. R., 2005, ApJ, 620, L9
 Ouchi M. et al., 2004, ApJ, 611, 685
 Ouchi M. et al., 2005, ApJ, 620, L1
 Page L. et al., 2007, ApJS, 170, 335
 Pettini M., Madau P., Bolte M., Prochaska J. X., Ellison S. L., Fan X., 2003, ApJ, 594, 695

Table A1. The same as Table 4, but for a Ly α line profile being a delta function at 10.2 eV. Small differences between observations are due to differences in the continuum flux within bandwidths.

Metallicity (Z_{\odot})	$f(m)$	$m_1, m_2(M_{\odot})$	$\frac{L_{Subz=5.7}}{L_{bol}}$	$\frac{L_{LALA}}{L_{bol}}$	$\frac{L_{Subz=6.56}}{L_{bol}}$	$\frac{L_{Subz=7}}{L_{bol}}$	$\frac{L_{ISAAC}}{L_{bol}}$
0	300 M_{\odot} δ -function	–	0.667	0.662	0.665	0.668	0.661
0	Heavy	100, 500	0.666	0.662	0.665	0.668	0.661
0	Larson, $m_c = 50M_{\odot}$	0.8, 150	0.673	0.668	0.671	0.674	0.667
0	Larson, $m_c = 10M_{\odot}$	0.8, 150	0.644	0.639	0.643	0.646	0.638
0	Salpeter	0.8, 150	0.603	0.598	0.601	0.604	0.597
1/50	Larson, $m_c = 50M_{\odot}$	0.8, 150	0.385	0.378	0.383	0.387	0.377
1/50	Larson, $m_c = 10M_{\odot}$	0.8, 150	0.362	0.354	0.359	0.363	0.353
1/50	Salpeter	0.8, 150	0.326	0.334	0.331	0.336	0.325
1	Larson, $m_c = 50M_{\odot}$	0.8, 120	0.218	0.209	0.215	0.220	0.207
1	Larson, $m_c = 10M_{\odot}$	0.8, 120	0.200	0.192	0.197	0.202	0.190
1	Salpeter	0.8, 120	0.182	0.174	0.179	0.184	0.172

Table A2. The same as Table 5, but for a Ly α line profile being a delta function at 10.2 eV.

Field	Redshift	$\frac{M_h}{L_{bol}} \frac{1}{\alpha_{esc} \epsilon^{1/\gamma}} (Z_{\odot} = 0)$	$\frac{M_h}{L_{bol}} \frac{1}{\alpha_{esc} \epsilon^{1/\gamma}} (Z_{\odot} = 1/50)$	$\frac{M_h}{L_{bol}} \frac{1}{\alpha_{esc} \epsilon^{1/\gamma}} (Z_{\odot} = 1)$
Subaru	5.7	57 – 81	31 – 46	17 – 26
LALA	6.55	~ 96 – 107	~ 53 – 60	~ 28 – 33
Subaru	6.56	51 – 67	28 – 38	15 – 22
Subaru	7.025	~ 60 – 67	~ 34 – 39	~ 18 – 22
ZEN	8.76	> 4.2 – 4.7	> 2.3 – 2.6	> 1.2 – 1.4
ISAAC ext	8.76	> 1.8 – 2.0	> 0.98 – 1.1	> 0.52 – 0.62

Press W.H., Schechter, P., 1974, ApJ, 187, 425
 Rhoads J.E. et al. 2003, AJ, 125, 1006
 Rhoads J.E. et al. 2004, ApJ, 611, 59
 Rhoads J.E., Malhotra S. 2001, ApJ, 563, L5
 Ryan-Weber E. V., Pettini M., Madau P., 2006, MNRAS, 371, L78
 Salpeter E. E., 1955, ApJ, 121, 161
 Salvaterra R., Ferrara A., 2003, MNRAS, 339, 973
 Salvaterra R., Ferrara A., 2006, MNRAS, 367, L11
 Santos M.R., 2004, MNRAS, 349, 1137
 Santos M. R., Bromm V., Kamionkowski M., 2002, MNRAS, 336, 1082
 Schaerer D., 2002, A&A, 382, 28
 Schaerer D., 2003, A&A, 397, 527
 Shimasaku K. et al., 2006, PASJ, 58, 313
 Sheth R.K., Tormen G., 2002, MNRAS, 329, 61
 Sheth R.K., Mo H.J., Tormen G., 2001, MNRAS, 323, 1
 Simcoe R. A., 2006, ApJ, 653, 977
 Songaila A., 2001, ApJ, 561, L153
 Spergel D.N. et al., 2007, ApJS, 170, 377
 Stark D.P., Loeb A., Ellis R., 2007, astro-ph/0701882
 Taniguchi Y. et al., 2005, PASJ, 57, 165
 Totani T., Kawai N., Kosugi G., Aoki K., Yamada T., Iye M., Ohta K., Hattori T., 2006, PASJ, 58, 485
 Tasitsiomi A., 2006, ApJ, 645, 792
 Verhamme A., Schaerer D., Masell A., 2006, A&A, 460, 397
 Willis J.P., Courbin F., 2005, MNRAS, 357, 1348
 Willis J.P. et al., 2006, New Astronomy Reviews, 50, 70
 Zaldarriaga M., 1997, PhRvD, 55, 1822